Hill, New York, 1954).
[34]This condition can be mathematically formulated by putting the shifted vibrational frequency $\omega_0+\alpha_v$ equal to zero. This gives $G(t)=\exp[i(\omega_0+\alpha_v)t]$; $G'(t)=G'(t)$, thus $G(t)\rightarrow G'(t)$.
[35]D. G. Hummer, Proc. Roy. Astron. Soc. 70, 1 (1961).
[36]S. Bhagavantam and A. V. Rao, Indian J. Phys. 8, 437 (1934).
[37]A. V. Rao, Proc. Indian Acad. Sci. 1, 274 (1935).
[38]H. L. Welsh, P. E. Pashler, and B. P. Stoicheff, Can. J. Phys. 30, 99 (1952).
[39]M. F. Crawford, H. L. Welsh, and J. H. Harrold, Can. J. Phys. 30, 81 (1952).
[40]A. I. Sokolovskaia, Proc. Lebedeev Phys. Inst. 27, 61 (1965).
[41]G. Döge, Z. Naturforsch. 23a, 1130 (1968).
[42]G. Döge, Z. Naturforsch. 23a, 1405 (1968).
[43]M. Scotto, J. Chem. Phys. 49, 5362 (1968).
[44]J. E. Clahill and G. E. Leroi, J. Chem. Phys. 51, 97 (1969).
[45]J. D. Masso, Y. D. Harker, and D. F. Edwards, J. Chem. Phys. 50, 5420 (1969).
[46]N. V. Zubova, N. E. Shalomeyeva, V. S. Gorelik, and M. M. Sushchinskii, Opt. i Spektroskopiya 27, 935 (1969) [Opt. Spectry. USSR 27, 508 (1969)].
[47]H. W. Kroto and J. J. C. Teixeira-Dias, Mol. Phys. 18, 773 (1970).
[48]C. H. Wang and P. A. Fleury, J. Chem. Phys. 53, 2243 (1970).
[49]M. Perrot, P. V. Huong, and J. Lascombe, J. Chim. Phys. 68, 619 (1971).

PHYSICAL REVIEW A VOLUME 4, NUMBER 3 SEPTEMBER 1971

Size of Quantized Vortex Rings in Liquid Helium II†

G. Gamota* and T. M. Sanders, Jr.
H. M. Randall Laboratory, University of Michigan, Ann Arbor, Michigan 48104
(Received 19 February 1971)

The energy dependence of the size of quantized vortex rings in He II is measured by studying the transmission of charged vortex rings through grids with holes of the order of a micron. A maximum-energy ring which can be transmitted is found for each hole size. These cutoffs are interpreted geometrically and lead to a relationship between ring size and energy which supports the quantization of circulation and the applicability of classical hydrodynamics to this problem. The circulation κ and core radius a of the rings are determined to be $\kappa=(1.002\pm0.03)\times10^{-3}$ cm^2 sec^{-1} and $a=(0.90\pm0.50)\times10^{-8}$ cm.

I. INTRODUCTION

A. General

The suggestion by Onsager[1] and Feynman[2] that circulation in superfluid liquid helium should appear in the form of quantized vortices and the discovery by Rayfield and Reif[3] that charged particles in liquid helium could produce and become attached to quantized vortex rings has stimulated a resurgence of interest in the subject of vortex motion. Rayfield and Reif, hereafter referred to as RR, found that the ion-vortex complex moved through the superfluid with a velocity related to its energy in precisely the manner predicted for a classical vortex in an ideal fluid, with the exception that the circulation was fixed at the value h/M as predicted by theory and with a core radius of atomic dimensions. Apart from the numerical values of these parameters—both determined by microscopic considerations—the behavior of the vortices was accounted for by equations derived nearly a century earlier. These early results had been worked out by Kelvin,[4] Thomson,[5] and others,[6] particularly in connection with a vortex theory of atomic structure.

The present experiment was designed as an independent test of the remarkable observation that classical equations, supplemented by a quantization condition, could give a quantitative description of a macroscopic quantum phenomenon.

B. Plan of Experiment

The present work, a brief account of which has appeared earlier,[7] concerns the physical size of vortex rings created by ions in superfluid helium. RR observed that at sufficiently low temperatures ions create quantized vortex rings, become bound to them, and convert work done electrically into hydrodynamic energy of the vortex ring. The bound charge provides a "handle" on the motion of a vortex ring and allows one to change its physical size by applying electric fields.

The equations describing the behavior of vortex rings in a perfect fluid predict that the size of a ring is approximately proportional to its energy but inversely proportional to its velocity. The exact equation to be used depends somewhat on the nature of the core of the vortex ring. For a hollow core,[8] for example, the classical equations are

$$E=\tfrac{1}{2}\rho\kappa^2R\left(\ln\frac{8R}{a}-2\right), \tag{1}$$

$$v = \frac{\kappa}{4\pi R}\left(\ln\frac{8R}{a} - \frac{1}{2}\right), \tag{2}$$

where E is the energy, v the translational velocity, ρ the fluid density, R the ring radius, a the core radius, and κ the circulation. If the core is not hollow, then the equations are the same except for a change in the value of the constant to the right of the logarithmic term in Eqs. (1) and (2).[8] Amit and Gross[9] derived quantum-mechanical equations where a de Broglie wavelength a_p appears within the logarithm. Their equations are

$$E = \frac{1}{2}\frac{h^2\rho_\infty R}{M^2}\left(\ln\frac{8R}{a_p} - 1.67\right), \tag{3}$$

$$v = \frac{h}{4\pi MR}\left(\ln\frac{8R}{a_p} - 0.67\right), \tag{4}$$

where ρ_∞ is the density of the fluid far away from the core and M is the mass of the helium atom.

RR used the classical equations and eliminated R, finding a relationship between v and E which represented their data extremely well. In this work we study the dependence of R on E. This is accomplished by studying the motion of the charged rings through screens with openings of known size. When the rings are smaller than the openings, a fraction will pass through the mesh, while no charged rings will be transmitted when the rings are larger than the holes. The size of the rings is controlled by the total potential through which the charged rings are passed. In the absence of friction and if the charge on a ring is the electronic charge, the total energy E is eV_T, where e is the electron charge and V_T the total potential difference. We thus sought a cutoff in current for a given size opening as V_T was varied. The data presented will consist of current-voltage (I-V) characteristics for various size grid openings.

II. EXPERIMENTAL TECHNIQUES

A. General

A recirculating He^3 cryostat is used to lower the temperature of the sample He^4 to about 0.3 °K. Such a low temperature is necessary in order to minimize frictional effects[3] and to consider the vortices to be quasifree. The sample chamber is filled by condensing high-purity He^4 gas which is passed through a charcoal trap cooled with liquid nitrogen.

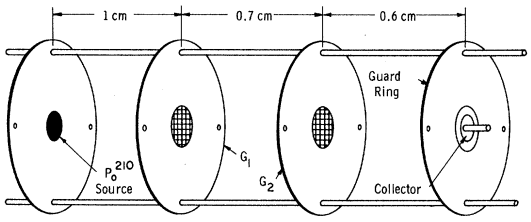

FIG. 1. Electrode structure.

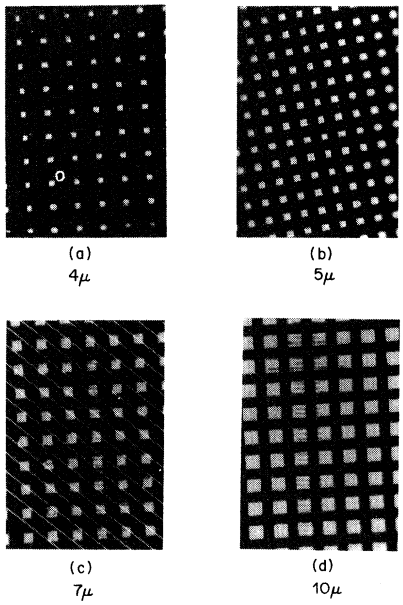

FIG. 2. Photomicrographs of a small region of each of the four grids. Fiduciary lines on (a) and (c) are separated by 10 μ.

B. Experimental Cell

The electrode structure is 3.1 cm in diameter and 2.3 cm long and is immersed in liquid helium in the sample chamber. A diagram of the structure is shown in Fig. 1. It consists of a Po^{210} radioactive source,[10] two grids, and a guarded collector. The source is fastened to a round gold-plated nickel disk by using a conducting Epoxy resin. The diameter of the source is $\frac{3}{16}$ in. and the inside diameter of the grid holders and the collector is $\frac{3}{8}$ in. The assembly is held rigid by insulated metal posts running through the disks. The mesh for the first grid G_1 is made from gold-plated tungsten wire 30 μ in diameter.[11] The grids G_2 are made from photoetched nickel mesh welded to a nickel washer.[12] The opening size of the grids was measured from photomicrographs taken from different regions of each grid. One photograph of each grid is shown in Fig. 2. The crosshairs in (a) and (c) are spaced by 10 μ; they are used to measure the openings, which are squares of side l. Values of l and the geometrical transmission coefficient τ are "4" grid $l = 3.86 \pm 0.25$ μ, $\tau = 0.053$; "5" grid $l = 4.85 \pm 0.30$ μ, $\tau = 0.155$; "7" grid $l = 7.25 \pm 0.40$ μ, $\tau = 0.180$; and "10" grid $l = 10.08 \pm 0.40$ μ, $\tau = 0.380$. The errors quoted are average deviations.

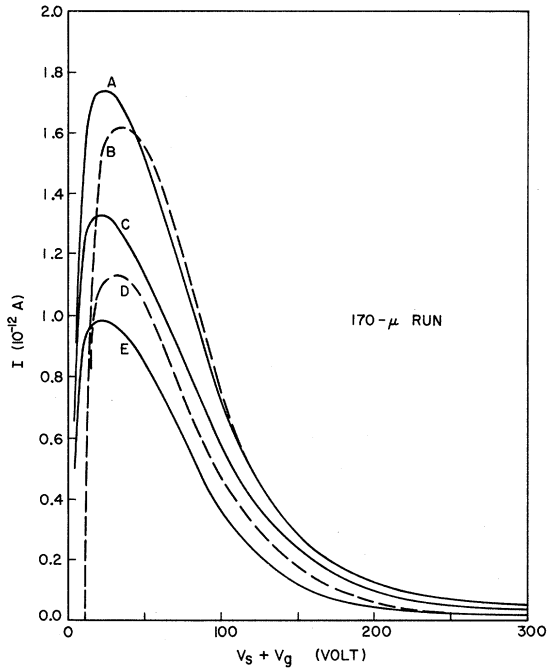

FIG. 3. I-V curves with grids 1 and 2 having 170-μ openings. The curves correspond to the following voltage settings: A – $V_s = +5$ V, $V_c = 0$; B – $V_s = +5$ V, $V_c = -10$ V; C – $V_s = +4$ V, $V_c = 0$; D – $V_s = +3$ V, $V_c = -10$ V; E – $V_s = +3$ V, $V_c = 0$.

C. Electronics

Three battery-operated power supplies are used in the experiment. A potential V_s is applied between the source S and grid G_1 to obtain ions of the desired polarity and to control the current density. In order to minimize space-charge effects, $|V_s|$ is usually kept below 5 V. A second voltage V_g is applied between G_1 and G_2. During the course of the experiment, this voltage is varied to change the size of the vortex rings. A third potential V_c exists between G_2 and the collector. Data are taken with both attractive and repulsive signs of V_c.

Electrical leads connect the grids and the feedthroughs soldered on top of the sample chamber flange. A coaxial cable[13] connects the collector with a feedthrough. The current is read by an electrometer[14] whose output is plotted against V_g on an X-Y recorder.

D. Data Acquisition

Current-voltage curves were obtained for the four small-opening grids in position G_2 and a separate run was made using a 170-μ grid for G_2. In each run V_s and V_c were kept constant while V_g was swept from 0 up to about ±300 V. The voltage sweep rate was slow, about 0.3 V/sec, in order to eliminate hysteresis effects and avoid distortion by filter time constants.

III. EXPERIMENTAL RESULTS

The I-V curves shown in Fig. 3 were obtained when both grids, G_1 and G_2, had 170-μ openings. These curves will prove useful for comparison with data obtained using small-opening grids. Curves A, C, and E were obtained with $V_c = 0$ and $V_s = +5$, $+4$, and $+3$ V, respectively ($+V_s$ indicates the creation of positively charged vortex rings). Curves B and D had $V_c = -10$ V and $V_s = +5$ and $+3$ V, respectively. In the latter case V_c was repulsive, so curves B and D show zero current until $|V_s + V_g| > |V_c|$. Such curves were used to determine the zero-current baseline.

Figures 4 and 5 show typical I-V curves for the several small grids under various conditions. The numbers 4–10 refer to the nominal size of the grid opening. The current maximum has been normalized to 1.0 to facilitate comparison of the curves.

Some general conclusions can immediately be stated. (i) Unlike the 170-μ case, the current in these curves apparently decreases to zero at some characteristic cutoff voltage which we will denote as V_k. The value of V_k is poorly determined from these graphs since the curves approach zero with zero slope, but the cutoff voltage appears to in-

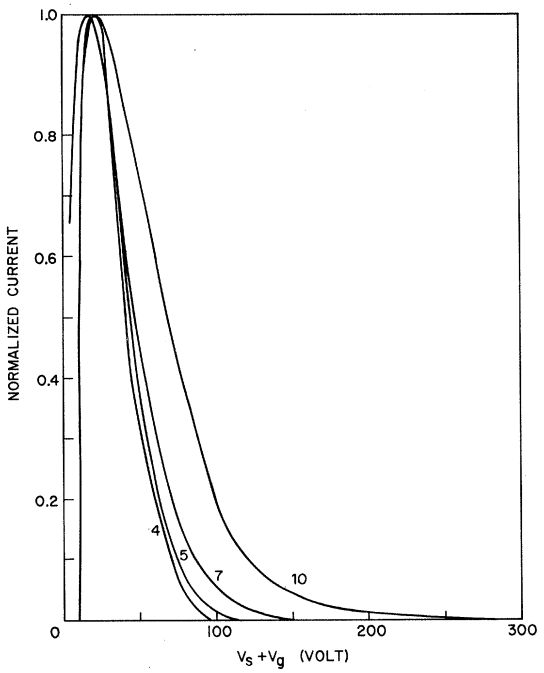

FIG. 4. Normalized I-V curves for positively charged vortex rings with grid 1 having 170-μ openings. The numbers labeling each curve indicate the opening size in grid-2 position. Curves 4 and 10 were taken with $V_s = +5$ V and $V_c = -10$ V, while curves 5 and 7 were taken with $V_s = +5$ V and $V_c = 0$.

crease with increasing opening size. (ii) Under no circumstance, e. g., attractive or repulsive V_c, does any detectable current reach the collector for voltages greater than V_k (the noise near cutoff is a few femtoamperes). (iii) At small voltages the curves are similar to those in Fig. 3 except for the magnitude of the current, which scales with the geometrical transmission coefficient. This is seen in Fig. 6.

IV. DATA ANALYSIS

A. Theoretical Considerations

It seems, from the data shown so far, that there is a cutoff voltage which depends on grid size, although a direct evaluation of it appears rather difficult. In this section we will show that a normalized plot of the square root of the current is much more useful in determining the cutoff point. The following argument suggests the usefulness of this type of plot.

Let us assume that a vortex ring is like a classical hoop of radius R that will pass through an aperture if and only if its core does not overlap an edge. Then for our case of square openings of side l, the fraction of rings t penetrating the mesh will be

$$t = \left(\frac{\text{effective area of hole}}{\text{total area of hole}}\right) \times \left(\frac{\text{open area}}{\text{total area}}\right) . \quad (5)$$

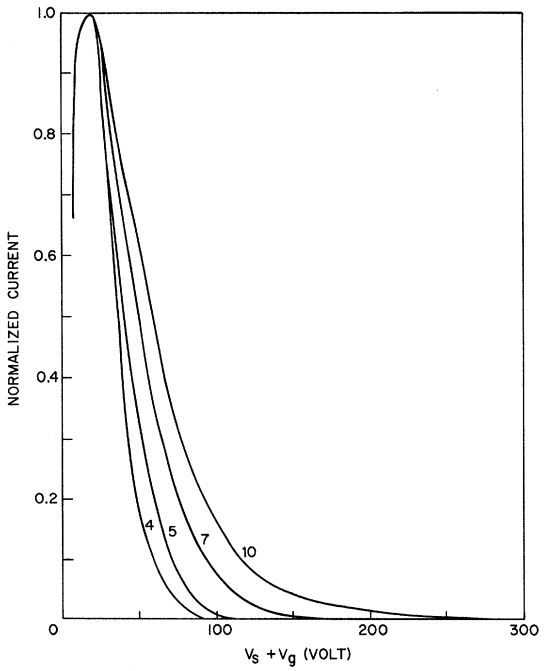

FIG. 5. Normalized I-V curves for negatively charged vortex rings with grid 1 having 170-μ openings. All curves were taken with $V_s = -5$ V and $V_c = 0$.

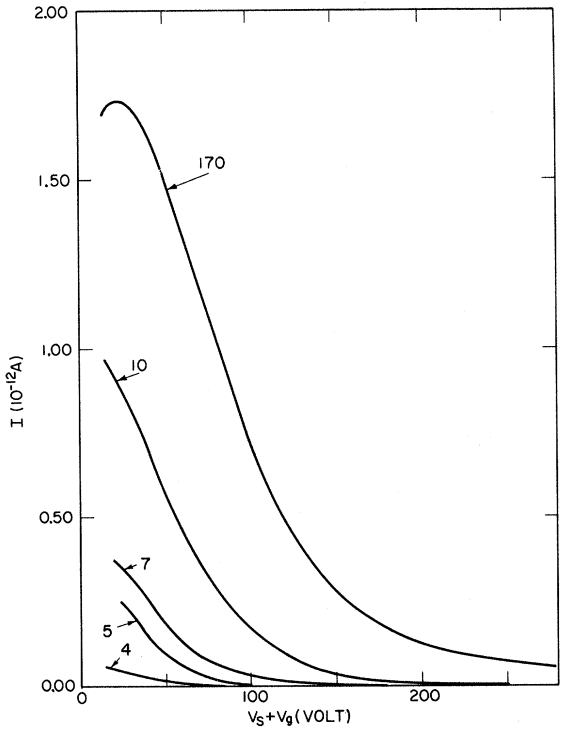

FIG. 6. Typical I-V curves for all grids in position G_2.

The first factor is easily seen from Fig. 7 to be equal to

$$(l - 2R)^2/l^2 = (1 - R/\tfrac{1}{2}l)^2 \quad \text{if } R \leq \tfrac{1}{2}l$$
$$= 0 \quad \text{if } R > \tfrac{1}{2}l . \quad (6)$$

The second factor is the geometrical transmission coefficient τ for the grid. We have assumed the planes of the rings and the mesh to be parallel, with the rings propagating in the direction normal to the mesh. Thus the transmission is proportional to the quantity $(1 - 2R/l)^2$ if $R \leq \frac{1}{2}l$, and is zero for

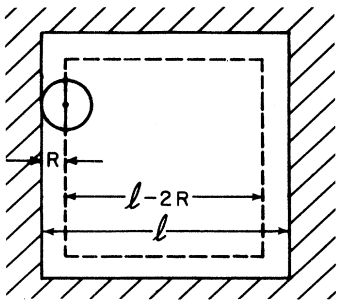

FIG. 7. Geometry of passage of a ring through a square hole of side l. The ring center must pass inside the dashed square of side $l - 2R$ if its core cannot encounter an edge.

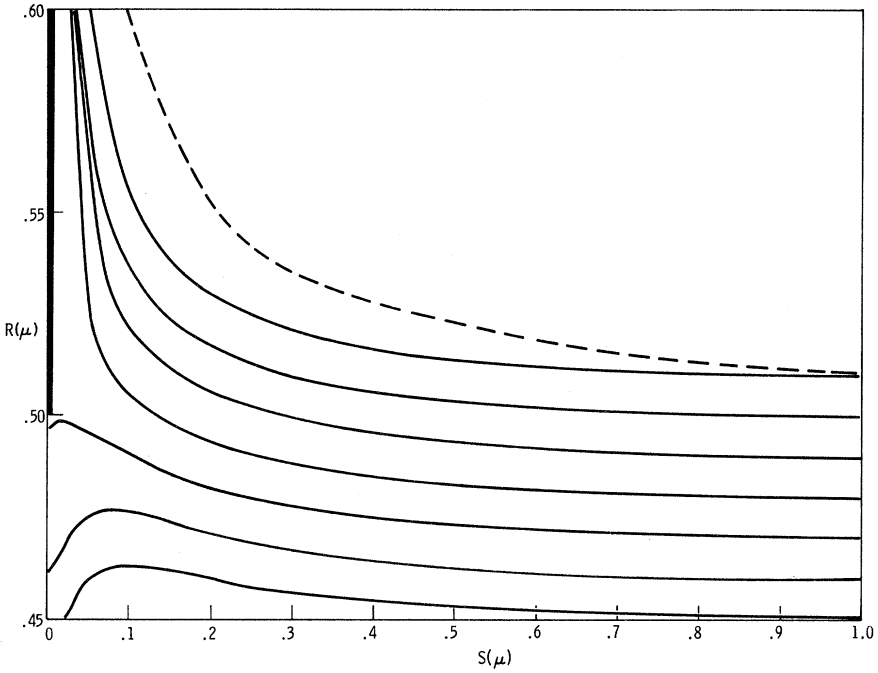

FIG. 8. Ring radius as a function of distance for rings approaching a wall with a 0.5-μ radius aperture. Curves are shown for incident radii, ranging from 0.45 to 0.51 μ. The dashed line represents the case when the aperture size is zero.

$R > \frac{1}{2}l$. As expected, the value of t goes over to the geometrical transmission coefficient τ of the grid when $R = 0$.

Let us now assume that this model is applicable for vortex rings whose radius R, by virtue of Eq. (1), is nearly proportional to the total "accelerating" voltage $V_T = V_s + V_g$. Equation (5) can thus be rewritten as

$$I = I_i\tau(1 - R/\tfrac{1}{2}l)^2 = I_i\tau(1 - V_T/V_k)^2 \quad \text{if } V_T \leq V_k$$
$$I = 0 \qquad \text{if } V_T > V_k\,. \tag{7}$$

I_i is the incident current, I the transmitted current, and V_k is the cutoff voltage, at which the vortex ring radius equals $\frac{1}{2}l$. We assume that the ring radius is much larger than the core and that frictional effects are negligible.

In applying Eq. (7) we assume that the radius of the vortex ring does not change as it approaches the aperture. This in fact is not true since hydrodynamic effects tend to enlarge it as it gets near a wall. Owing to the complexity of the problem, we have not analyzed the actual situation encountered in the experiment, but have solved approximately the simpler problem of a single ring approaching coaxially a round aperture in a wall. The details of the calculation have been given elsewhere,[15] but briefly the method of solving the problem is as follows: A vortex ring of radius R_0 approaches a wall. The velocity field is identical with the magnetic field which would be produced by a current loop near a superconducting wall. In the latter problem a distribution of current would be induced in the wall. In the hydrodynamic case we can speak of a distribution of vorticity induced in the wall. We calculate the induced vorticity from the requirement that the boundary conditions at the plane be satisfied, and then compute the effect of the induced vorticity on the motion of the ring. The method

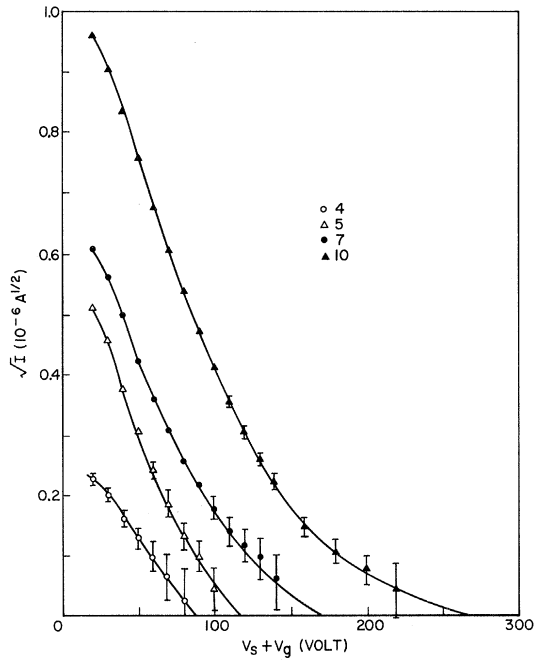

FIG. 9. Square root of the current vs voltage.

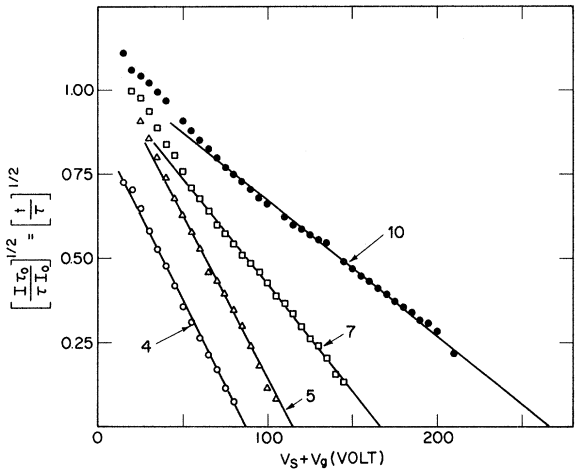

FIG. 10. Normalized plot of the square root of the current vs voltage, as explained in text. The data points are a result of digitizing the original curves. Plausible straight lines have been drawn through each set of data.

can be checked in the limiting case of vanishing aperture size, where the problem can easily be solved by the method of images.

The results are shown in Fig. 8, where we plot the radii R of various vortex rings as a function of their distances from the aperture in the wall. The plots show that the radii do grow as the rings get closer to the wall, their growth depending on the ratio of the radius at infinity to the aperture size. Small rings get through with only a slight interaction and only rings very close to the aperture size and larger do not pass through. An exact solution to this problem has appeared recently[16] and it is consistent with ours within our expected accuracy. We find that if the ratio of the initial ring radius to the aperture radius is greater than about 0.94, no ring will pass through the hole. From this we conclude that within experimental error no correction to Eq. (7) is justified.

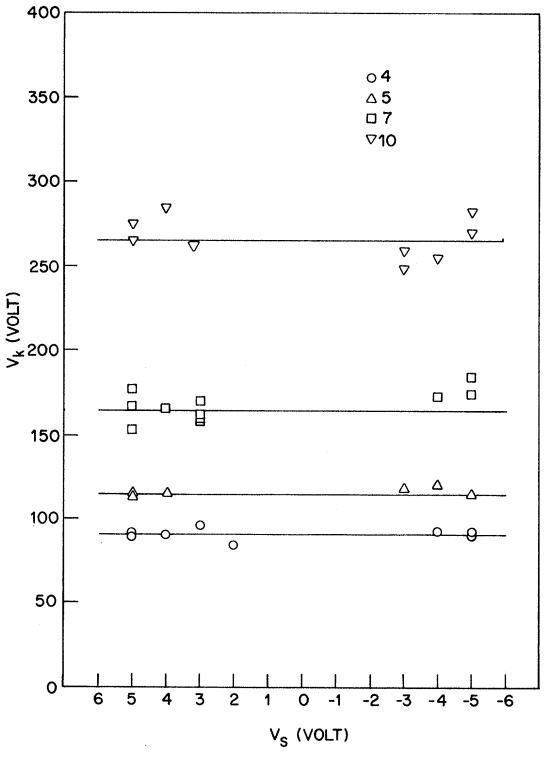

FIG. 11. Cutoff voltage V_k vs source voltage V_s. The horizontal lines are average values of V_k for each grid size.

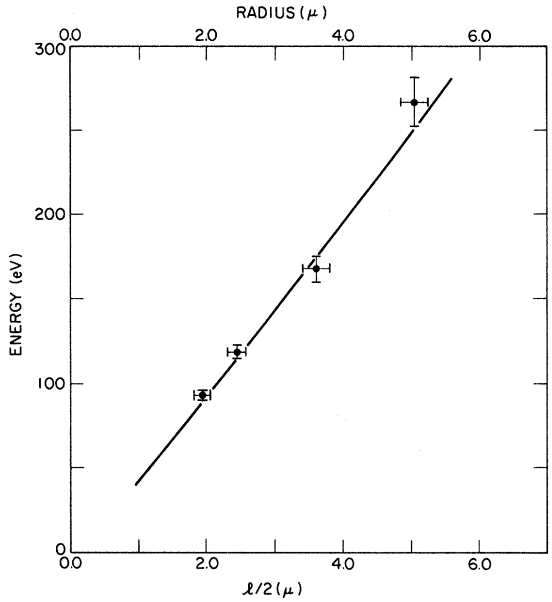

FIG. 12. Cutoff energy E_k vs opening size. The points are experimental. The solid line is a plot of Eq. (1) using the least-squares best-fit values of κ and a. A curve drawn using RR parameters would not be discernibly different.

B. Reduction of Data

One can now find V_k by plotting $I^{1/2}$ vs V_T (Fig. 9) and locating the point where the current goes to zero. Cutoff should be approached with a finite slope in such a plot, but the data will not lie on a straight line unless I_t is constant. The plots are not straight, and the reason is that the current incident on the second grid G_2 does not remain constant as V_g is varied, as is evident from the 170-μ data of Fig. 3. To overcome this problem we normalize all data from the small grids to the 170-μ case. We assume that the current transmitted by the 170-μ grid (I_0) is equal to the current incident on a small grid under identical operating conditions, except for the fact that the geo-

TABLE I. Tabulation of the core radius using the experimental values of E_k, $\frac{1}{2}l = R_k$, and $\kappa = 1.00 \times 10^{-3}$ cm^2/sec in Eq. (1). The upper and lower bounds on a are obtained from the error limits in E_k and R_k.

E_k(eV)	$R_k(\mu)$	a(Å)
		<1.80
93±3	1.93±0.12	0.72
		>0.20
		<1.80
119±4	2.42±0.15	0.72
		>0.20
		<5.3
168±8	3.63±0.20	2.00
		>0.58
		<1.80
267±15	5.04±0.20	0.60
		>0.18

metrical transmission coefficient τ_0 of the 170-μ grid is less than 1. Thus the current incident on the second grid is $I_i = I_0/\tau_0$, and $t = I/I_i = (I/I_0)\tau_0$ is the transmission coefficient of a small grid for vortices.

If all is consistent then a plot of $(t/\tau)^{1/2}$ vs V_T should yield a straight line crossing the voltage axis at the point V_k, and approaching $(t/\tau)^{1/2} = 1$ for small voltages. Figure 10 shows some typical data reduced in this manner. The plots do have the expected characteristics. They are approximately straight lines, yielding well-defined cutoff voltages, and approaching $(t/\tau)^{1/2} = 1$ for small voltages. Cutoff voltages thus determined are plotted against source voltage in Fig. 11. The data fall nicely into four groups, characterized by the grid size, and within experimental error the cutoffs are independent of V_s.

In Fig. 12 we plot the cutoff energy $E_k \equiv e V_k$ against the grid size $\frac{1}{2}l$. The vertical error bars represent the average deviations of several independent determinations of E_k using different values of V_s, V_c, and polarity. The error bars on the opening size are also average deviations and are based on the measurements discussed previously.

V. INTERPRETATION OF DATA

We see from the points plotted in Fig. 12 that there is a monotonic relationship between the cutoff energy and grid size. Let us now assume that at cutoff the radius of the vortex ring is given by $R_k = \frac{1}{2}l$, and use Eq. (1) to compare theory and experiment by adjusting the parameters κ and a. The solid line in Fig. 12 is a plot of Eq. (1) using the least-squares best-fit values

$$\kappa = (1.002 \pm 0.030) \times 10^{-3} \text{ cm}^2/\text{sec}, \quad a = 0.9 \pm 0.5 \text{ Å}.$$

The value of the circulation is in very good agreement with RR's value $\kappa = (1.000 \pm 0.002) \times 10^{-3}$ cm^2/sec, from a $v(E)$ curve, and supports the notion that only singly quantized vortex rings are observed One quantum of circulation is

$$\kappa = h/M = 0.997 \times 10^{-3} \text{ cm}^2/\text{sec}.$$

Our value of the core radius is within experimental error of RR's number ($a = 1.28$ Å) but we note in Table I that three of the four points indicate a value of a about one-half that reported by RR, but in agreement with Amit and Gross's estimate of a_p. However, owing to the scarcity of experimental points and the error in each, we cannot claim an accurate determination.

We have avoided any discussion of the shape of the I-V curves, for such a study was not needed for the interpretation of the cutoff voltages. Study of the behavior of vortex ring beams and the I-V curves are interesting subjects, which will be discussed elsewhere.[17]

VI. CONCLUSIONS

The experimental results reported here show that the physical size of charged quantized vortex rings can be calculated from the classical equation relating energy and radius. The data lend support to the quantization of circulation, and to the notion that only singly quantized rings are seen. We also have shown that the encounter of a charged ring with a grid can be interpreted to a sufficient approximation by a simple geometrical picture.

†Work supported in part by the U. S. Atomic Energy Commission.

*Present address: Bell Telephone Laboratories, Murray Hill, N. Y. 07974.

[1]L. Onsager, Nuovo Cimento Suppl. 6, 249 (1949).

[2]R. P. Feynman, in *Progress in Low Temperature Physics*, edited by C. J. Gorter (North-Holland, Amsterdam, 1955), Vol. 1, Chap. II.

[3]G. W. Rayfield and F. Reif, Phys. Rev. Letters 11, 305 (1963); Phys. Rev. 136, A1194 (1964).

[4]W. Thomson (Lord Kelvin), in *Mathematical and Physical Papers* (Cambridge U. P., Cambridge, England, 1910), Vol. IV, p. 13.

[5]J. J. Thomson, *A Treatise on the Motion of Vortex Rings* (MacMillan, London, 1883).

[6]A summary of the early work on vortices can be found in A. B. Basset, *A Treatise on Hydrodynamics* (Dover, New York, 1961), Vol. II, Chap. XIV.

[7]G. Gamota and T. M. Sanders, Jr., Phys. Rev. Letters 15, 949 (1965).

[8]Reference 6, p. 87; see also, P. H. Roberts and R. J. Donnelly, Phys. Letters 31A, 137 (1970).

[9]D. Amit and E. P. Gross, Phys. Rev. 145, 130 (1966).
[10]The Po^{210} was purchased from U. S. Radium Corp. and the activity at time of purchase was 750 μCi/in.^{2}
[11]The 170-μ grids were from 2C39A tubes and were purchased from Eimac Corp.
[12]The mesh with different size openings was purchased from Buckbee Mears Co.
[13]Model 250-3919, Microdot Corp.
[14]Model 610BR Electrometer, Keithley Corp.
[15]G. Gamota, Ph. D. dissertation (University of Michigan, 1966) (unpublished).
[16]A. Walraven, Phys. Rev. A 1, 145 (1970).
[17]G. Gamota (unpublished).

PHYSICAL REVIEW A VOLUME 4, NUMBER 3 SEPTEMBER 1971

Exchange Interaction in Solid He^3

C. Ebner and C. C. Sung
Department of Physics, The Ohio State University, Columbus, Ohio 43210
(Received 5 March 1971)

On the basis of our previous theory used to calculate the static properties of crystalline He^3 and He^4 at $T=0$, we compute the exchange interaction of the nuclear spins in bcc He^3 as a function of molar volume, obtaining good agreement with experiment. Comparison with the theories of Nosanow and co-workers and of Guyer and Zane shows that the success of the theory is mainly due to the effective-force constant used in the computations.

I. INTRODUCTION

In recent years the exchange interaction J between two atoms in solid He^3 has been measured by a number of workers.[1–5] The absolute value of J ranges from about[6] 10^{-3} to 10^{-4} °K as the nearest-neighbor distance a runs from 3.7 to 3.5 Å corresponding to molar volume between 23.5 and 19.9 cm^3 in the bcc phase. These values of J are large compared to what one would predict for a classical crystal because of the large zero-point motion of the relatively light He^3 atoms. However, J is still very small compared to the ground-state energy E_0 which is of order 1 °K per particle and consequently the possibility of exchange may be ignored in calculations of E_0 and related thermostatic quantities. This is done in most theories of quantum crystals and was done by us in Ref. 7 where the thermostatic properties of crystalline He^3 and He^4 are calculated at $T=0$. In the present work we evaluate the exchange interaction as a function of molar volume on the basis of the theory and results of Ref. 7.

A theoretical determination of J was first given by Bernardes and Primakoff[8] and subsequently by Mullin, Nosanow, and co-workers.[9–11] In addition, Guyer and Zane[12] have recently calculated J, basing their work on the quantum crystal theory of Guyer[13] and Sarkissian.[14]

The approach that we use is similar to that of the previous theories; J is defined in terms of the energy difference between the singlet and triplet spin states of two nearest-neighbor He^3 atoms. There are, however, important differences among the three approaches as regards the formalism and the approximations used in computing this energy difference; these are discussed below.

The calculation of J is an important one because J is extremely sensitive to the force constant α describing the single-particle effective potential in which each atom sits, and there is also some sensitivity of the result to the form of the two-particle correlation function. Thus J should be a good test of any quantum crystal theory. In this context it should be mentioned that there is some disagreement among experimental values of J which are obtained from several different types of experiment. In particular, the values inferred from NMR measurements are sensitive to small concentrations of impurities. Reference 5 contains a discussion of this problem.

The remainder of this paper contains (i) in Sec. II, a brief review of the formalism of Ref. 7 and construction of symmetric and antisymmetric space states for nearest neighbors; (ii) in Sec. III, the calculational details and numerical results; and (iii) in Sec. IV, a discussion of our results and a comparison of them with experiment and other theories.

II. FORMALISM

We begin by summarizing the theory of Ref. 7 in which exchange effects are ignored and the particle statistics play no role. The single-particle Green's function for the He^3 localized at position $\vec{R}_i$ is given by[15]

$$g_i(1,1';\nu)=\sum_\rho \phi_{i\rho}(1)\phi_{i\rho}(1')/(\omega_\nu-\epsilon_\rho) \quad (1)$$

in the frequency representation. The single-particle wave function $\phi_{i\rho}(1)$ obeys the equation

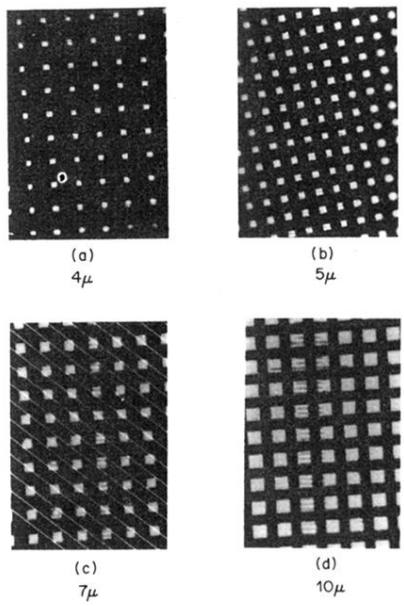

FIG. 2. Photomicrographs of a small region of each of the four grids. Fiduciary lines on (a) and (c) are separated by 10 μ.